Astron. Astrophys. 329, 613–623 (1998)

ASTRONOMY
AND
ASTROPHYSICS

Helium enhancements in luminous OB-type stars: the effect of microturbulence⋆

N.D. McErlean[1], **D.J. Lennon**[2], **and P.L. Dufton**[1]

[1] The Department of Pure and Applied Physics, The Queen's University of Belfast, Belfast BT7 1NN, Northern Ireland
[2] Institut für Astronomie und Astrophysik der Universität München, Scheinerstrasse 1, D-81679 München, Germany

Received 14 July 1997 / Accepted 28 August 1997

Abstract. We present non-LTE analyses of high quality spectra for two B-type supergiants, κ Orionis & ϵ Orionis (spectral types B0.5 Ia & B0 Ia respectively). We investigate the effect of including a microturbulent velocity in the H I, He II and He I line broadening on the derived stellar atmospheric parameters ($T_{\rm eff}$, $\log g$ and y). Its inclusion has a significant effect on the profiles of the lines of neutral helium and leads to approximately *normal* estimates for the helium fractional abundances for both supergiants. By contrast, adopting zero microturbulence implies significant helium overabundances, *if* we adopt the mean abundance of all the lines considered here. The He I lines at 4437, 4387 and 5047Å are found to be rather insensitive to microturbulence and hence are more reliable indicators of helium abundance. There are some remaining unresolved discrepancies, such as a systematic difference between singlet and triplet transitions which we attribute to the neglect of line blocking, while the 5015Å 2^1S – 3^1P transition remains much stronger than predicted. This latter problem we tentatively attribute to the neglect of sphericity; the generalized dilution effect discussed by Voels et al. (1989). We suggest that a judicious choice of He I lines, and the use of an appropriate microturbulent velocity, may contribute to resolving the 'helium discrepancy' in O-type stars. The question of the origin of a perceived microturbulence in supergiants is also briefly discussed in the context of stellar winds.

That two normal supergiants have close to solar helium abundances clearly implies that they have *not* undergone dredge-up in a previous red supergiant phase of evolution, supporting the contention that massive stars do not perform blue loops in the HR diagram at solar metallicity. Marginal evidence for a mild helium overabundance in κ Ori however could be interpreted as being due to mixing processes, perhaps during its main sequence lifetime.

Key words: stars: atmospheres – stars: early-type – stars: evolution – stars: supergiants

Send offprint requests to: N.McErlean@qub.ac.uk

⋆ Based on Observations collected at the European Southern Observatory, La Silla, Chile

1. Introduction

There are a number of important theoretical uncertainties, for example the treatment of convection processes, mass loss and rotation, concerning the evolution of massive stars. Such processes generally lead to varying degrees of surface contamination by nucleosynthetically produced material from the stellar interior (see Maeder & Meynet 1989 for example). Therefore the surface chemical composition of massive early-type stars is a vital diagnostic tool for understanding their evolution. Blue supergiants in particular may be considered as key tests of stellar evolution since neither their very distribution in the Hertzsprung-Russell diagram, nor their number ratio relative to red supergiants, both as a function of metallicity, are accounted for by theory (for recent discussions of these problems see Maeder 1994 and Langer & Maeder 1995). It is therefore vital that reliable surface abundances be obtained for such stars, in particular for the elements helium, carbon, nitrogen and oxygen (see also Fliegner et al. 1996 for a discussion of the importance of boron).

For O- and early B-type stars, one is in the fortunate position of having access to profiles of *both* neutral and ionised helium lines, which, together with the hydrogen Balmer lines, may be used to estimate the helium abundance simultaneously with the surface gravity and effective temperature. There have been a number of previous analyses using plane-parallel non-LTE models. For example, Voels et al. (1989) used wind-blanketed models to analyse four stars of spectral type O9.5 that form a sequence in luminosity class (Ia, Ib, II, V). They found an enhanced helium fraction, y, of 0.18±0.03 by number, only for their most luminous Ia supergiant, α Cam. Lennon et al. (1991) also found enhanced helium abundances for the B0.5 Ia supergiants κ Ori, Sk−68° 41 and Sk 159 (y = 0.20, 0.23 & 0.35 respectively). More recently, Herrero et al. (1992) analysed a sample of 25 Galactic luminous O-type stars, finding enhancements for approximately half of these objects. Finally, Smith & Howarth (1994), in their analysis of three O9.5 Iab supergiants, gave evidence for more marginal helium enhancements and a correlation with the stars' CN abundances.

A common problem encountered in this previous work was that a consistent fit to all the available He I lines could not be

obtained for a given helium abundance. Voels et al. (1989) attributed this to the extended spherical nature of the supergiant photosphere leading to a strengthening of triplet absorption lines relative to singlet lines – the so-called 'generalized dilution effect'. They therefore gave greatest weight to the weakest lines, which they argued formed deeper in the atmosphere where extension (and wind) effects are less important. Smith & Howarth (1994) used the same line of argument in their analysis of O9.5 supergiants and it is noticeable that both these papers derive only moderate helium enrichments compared to the results of Lennon et al. (1991), where more substantial overabundances are found. These latter authors however adopted a mean abundance from all lines considered, but commented in detail on the difficulties involved in obtaining a consistent fit for all the He I lines, a problem which was further elaborated upon by Lennon (1994). All these analyses however have neglected the effect of microturbulence on the line formation process, despite the fact that microturbulent velocities comparable to the sound speed are consistently deduced from analyses of metal lines in B-type supergiants (see, for example, Lennon et al. 1991).

2. Microturbulence in early-type stars

It was recognised very early on in the analysis of the spectra of early-type stars, that some additional broadening mechanism, other than thermal or intrinsic, was required to explain the observed widths and strengths of metal lines. This became evident through comparing the relative strengths of lines within a multiplet in dwarfs and supergiants and, using curve of growth arguments, Struve & Elvey (1934) first postulated that this broadening and strengthening of lines might be caused by small-scale turbulent velocities. Subsequently, LTE analyses confirmed these findings, with typical microturbulent velocities of order 5 kms^{-1} being found for the main sequence B-type stars (Hardorp & Scholz 1970) while even higher values, of order 20 – 30 kms^{-1}, were obtained for supergiants (Lamers 1972, Dufton 1972, Lennon & Dufton 1986). The magnitude of these estimates decreased with the introduction of non-LTE techniques; for example Mihalas (1972) showed that the observed strength of the Mg II 4481Å doublet in early B-type main sequence stars could be reproduced with zero microturbulence. For supergiants however, values close to the speed of sound were still obtained. Lennon et al. (1991) adopted v_t = 10 kms^{-1} in their non-LTE analysis of 3 supergiants, noting that even this value was insufficient to remove the slope in their abundance–equivalent width plots. More recently, Smartt et al. (1997) analysed 4 Galactic supergiants (using methods similar to ours) and found that v_t = 30 kms^{-1} was appropriate for both LTE and non-LTE. Gies & Lambert (1992) analysed a sample of 39 B-type stars (of which 3 were supergiants) in both LTE and non-LTE. They found that the assumption of LTE led to very large microturbulences (typically 25 to 30 kms^{-1}) for their supergiants, whereas a non-LTE analysis yielded smaller values (typically 10 kms^{-1}). Significantly, there are very few microturbulence estimates for O-type stars from photospheric metal lines due to the lack of suitable lines; see for example Peterson & Scholz (1971).

The fact that supergiants have significant winds led naturally to the suggestion that microturbulence might, to a large extent, be the result of an outflow (Kudritzki 1992, Lamers & Achmad 1994). However, it is interesting to note that recent detailed non-LTE investigations of main sequence B-type stars, with mass-loss rates much lower than supergiants, imply that microturbulent velocities as high as 10 kms^{-1} are applicable (Gies & Lambert 1992, Kilian et al. 1991). Further, it is found that microturbulence is *necessary* to fit even stellar wind line-profiles in OB-type stars (Groenewegen & Lamers 1989, Haser et al. 1995, McCarthy et al. 1997), although this has been linked to the presence of shocks in the wind. The aim of this paper is to investigate how the inclusion of microturbulence, in the classical sense, might modify the helium abundance results discussed above. It is motivated in part by our involvement in a systematic spectroscopic analysis of a sample of B-type supergiants in our own Galaxy and in the SMC (McErlean et al. 1997, Lennon 1997). Here we present atmospheric parameters (T_{eff}, $\log g$ and helium fraction, y) for two representative and well studied Galactic objects, κ and ϵ Ori, as well as the results of numerical tests performed to investigate the effect of microturbulent velocities on the line profiles of hydrogen and neutral and ionised helium.

3. Spectroscopic data and non-LTE methodology

The spectra analysed in this paper were obtained using the ESO 3.6–m telescope and the Cassegrain–echelle spectrograph (CASPEC) with a Tektronix 512x512 27μm pixel CCD detector. The short camera was used with the 31.6 lines/mm echelle grating and a 2 arcsec slit resulting in a spectral resolution of $\sim$ 20 000 in the wavelength region covered, which was approximately 3830–5240Å. A formal signal-to-noise ratio in excess of 100 was obtained but unexpected fringing, probably due to the use of neutral density filters, was found to be present in the observations. This was most serious in the observations of ϵ Ori and increased towards the red, reaching 2% of the continuum level at around 5000Å. The echelle spectra were extracted, background corrected and rectified within the MIDAS environment (Ponz & Brinks, 1986) using standard techniques. The individual, normalised exposures were co-added and transferred to the DIPSO environment (Howarth & Murray 1991), where equivalent width measurements and line fitting were performed.

The analyses presented here are based upon non-LTE model atmospheres and non-LTE line formation computations; further details may be found in McErlean et al. (1997) and Lennon et al. (1991). Briefly, the model atmospheres used include the elements hydrogen and helium, and permit departures from LTE for the first five levels of H I and He I, and the first ten levels of He II. We note that for He I, the splitting of the states due to spin and angular momentum was ignored with these levels being treated as purely hydrogenic.

The subsequent line formation calculations were performed using the programs DETAIL and SURFACE (Giddings 1981 and Butler 1984, respectively), with the former solving the radiative transfer and statistical equilibrium equations and the latter com-

puting the emergent flux. For these calculations the number of non-LTE levels was increased to 10 levels for H I, 27 levels for He I (including the explicit treatment of all LS-states up to and including n=4; states n=5 to n=8 have their spin series treated as degenerate) and 14 He II levels. As pointed out by Lennon et al. (1991), the use of hydrogenic levels above n=4 for neutral helium may be inadequate, as these states are the upper levels for many of the transitions considered in this paper.

Line formation calculations were performed for helium fractions of y = 0.1, 0.2 (Throughout this paper, the definition y = N[He] / N[H + He] is used). We have allowed for the effect of microturbulence on the line profile in the standard way by including an additional term in the usual Doppler width ($\Delta\lambda_{\rm D}$);

$$\Delta\lambda_{\rm D} = \frac{\lambda_0}{c}\sqrt{v_{th}^2 + v_t^2} \quad (1)$$

where v_{th} is the thermal velocity of the ion in question and v_t is the microturbulent velocity. This modified Doppler profile is then convolved with the usual Stark profiles. As we pointed out however, the line formation calculations were performed in two steps. In the first step (DETAIL) we solved for the level populations (or departure coefficients) using purely Gaussian profiles for all lines, detailed numerical profiles only being included in the final profile calculations (SURFACE). Typically in non-LTE calculations of this kind for main sequence B-type stars, microturbulence is only included in the final profile calculation since the effect of values up to 5 kms^{-1} on the level populations is small (Kamp 1978, Mihalas 1972). However, for supergiants we have to consider values in excess of 10 kms^{-1} and test calculations showed that significantly different profiles resulted if the microturbulence was also included in the computation of the level populations. Similar results were found for Mg II by Snijders & Lamers (1975, see their Table 2). We have therefore adopted the same value of microturbulence in *both* DETAIL and SURFACE in all the line formation calculations discussed here.

4. Analysis

A preliminary examination of the synthetic line profiles showed that the value of microturbulence, v_t, had little effect on the profiles of the hydrogen lines. This is to be expected since the thermal velocities of the hydrogen ions are higher than our typical microturbulent velocities and any small differences are masked by the large intrinsic Stark broadening. The ionised helium lines also showed little dependence on microturbulence. In this case, although the thermal velocities are comparable to v_t, the lines are very weak and close to the linear part of the curve of growth. There is therefore only a small dependence which is again masked by the strong Stark profiles. An exception is the strongest He II line at 4686Å, which has a more strongly developed Doppler core (relative to the Stark wings) than the lines at 4200 and 4542Å. However, in the case of the stronger neutral helium lines, some very significant changes in both line profile and equivalent width were found. It might be expected therefore, that the parameters derived predominantly from H I and He II lines (namely $T_{\rm eff}$ and $\log g$) would be insensitive to the adopted microturbulence, while the derived helium fraction would depend on this parameter.

In order to investigate the consequences of these changes in the line profiles, we have estimated atmospheric parameters ($T_{\rm eff}$, $\log g$ and y) for ϵ Ori (B0 Ia) and κ Ori (B0.5 Ia), initially adopting a zero microturbulent velocity, and then relaxing this constraint by using a value estimated from the metal lines. This procedure should be valid if the metal lines form at depths comparable to the helium lines and we discuss this point further below.

All synthetic profiles were convolved with both a Gaussian filter to account for instrumental broadening, and a rotational velocity broadening function (80 & 90 kms^{-1} for κ Ori & ϵ Ori respectively – as determined from their metal line profiles). Our analysis is similar to that described in Lennon et al. (1991), whereby a simultaneous estimation of $T_{\rm eff}$, $\log g$ and y is sought.

4.1. Hydrogen and helium lines considered

The He II lines at 4200, 4542 and 4686Å were observed in both stars. However, the usefulness of the line at 4686Å may be compromised by wind emission (see Gabler et al. 1989, Lennon et al. 1991, Herrero et al. 1992) and hence it was not used as a temperature indicator. The line at 4199.83Å is also affected by absorption due to N III at 4200.02Å (as noted by Smith & Howarth 1994 and as shown in Fig. 2), while that at 4542Å appears to be unaffected by such problems and hence was given highest weighting in our fitting procedure.

Our spectra include the Balmer hydrogen lines Hβ, Hγ, Hδ, Hϵ, H6 and H7. Hβ is often affected by core emission from the stellar wind and this effect was observed in our spectra, while Hϵ was also excluded due to the presence of an interstellar line of calcium in its blue wing. The higher lines in the Balmer series were rejected as they are close to the blue edge of our spectra and had lower signal to noise ratios. Therefore we have used Hγ and Hδ as gravity indicators, in all cases giving greater priority to Hδ, which is less affected by blending with metal lines.

Neutral helium lines were available at 4026, 4387, 4437, 4471, 4713, 4922, 5015 and 5047Å and we have tried to fit this set in its entirety. (4009 & 4121Å were also observed. The former was excluded as our line profile computations did not include it while the latter was not used due to blending problems associated with lines of O II.)

4.2. The value of microturbulence

The microturbulent velocity was estimated from the relative strengths of metal lines with the species O II, N II and Si III being considered. Having determined preliminary atmospheric parameters from the hydrogen and helium spectra, the microturbulence, v_t, was freely varied in order to ensure that the derived abundances were not a function of strength (using a method very similar to that described in Smartt et al. 1997). The close proximity of many of the O II lines led to blending problems and poorly resolved features were not considered. For N II lines, only the lines at 3995, 4236 & 4242Å were resolved, and hence this

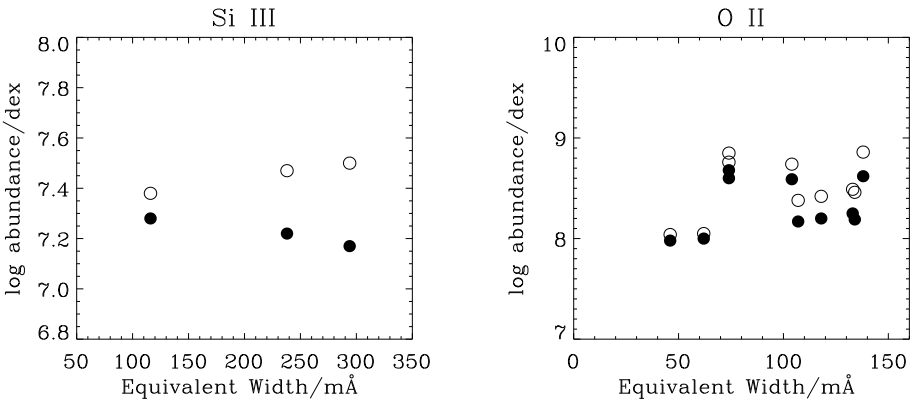

Fig. 1. Logarithmic abundance vs. equivalent width for ϵ Ori. (Results for κ Ori were similar.) In the Si III plot, the open circles represent v_t = 10 kms^{-1} and the filled circles represent v_t = 15 kms^{-1}. In the O II plot, the open circles represent v_t = 10 kms^{-1} and the filled circles represent v_t = 20 kms^{-1}. See text for further discussion.

species was not used to estimate the microturbulence. By contrast, the Si III multiplet near 4560Å had three well-resolved lines covering a substantial range in line strength, with good quality line-strength measurements.

The abundance – equivalent width plots for ϵ Ori are presented in Fig. 1. A considerable scatter is found in the abundance estimated from lines due to O II. Also we note that for this ion, any single multiplet has a small range in equivalent width and hence the value of v_t is not well constrained. Therefore, whilst the lines of oxygen taken as a whole indicate a large microturbulence (of greater than 20 kms^{-1}), errors inherent in our plot (that may be due to atomic data errors or inadequate allowance for non-LTE effects) prevent our making any definite conclusions. The Si III lines, which come from a single multiplet, imply a microturbulent velocity of v_t = 12 kms^{-1} for both κ and ϵ Ori (with an error estimate of $\pm$3 kms^{-1} probably being appropriate) and this value is adopted in the subsequent H and He line calculations. Comparing the depth of formation of the silicon lines (see Fig. 5) we see that they form at depths comparable to the He I lines at 4387, 4713, 5047 and 4437Å. Thus our procedure should be adequate for these lines, but may possibly underestimate v_t for those lines forming further out in the wind, if microturbulence does in fact mimic the effects of the wind.

5. Results

Our analysis procedure was as follows: we have determined effective temperatures and gravities for each supergiant for our two model helium abundances. These are listed in Table 1 – the number of significant figures provided are to illustrate the dependence of these quantities on the helium fraction and are not representative of the likely errors. For both stars, increasing the helium abundance reduces our estimate of the gravity which in turn reduces that for the effective temperature. As was implied by the synthetic profiles, our temperature and gravity estimates were effectively independent of the value adopted for the microturbulent velocity.

The He I lines have been calculated using the appropriate values of the atmospheric parameters for each value of y. In Table 2 we show the estimates of helium fraction, while in Figs. 3 and 4 we present our spectral line fits. The extrapolated values were obtained by linearly extrapolating the helium line profiles beyond the limits of our grid. In some cases (marked with a dagger) the extrapolation was relatively small and the estimates should be useful; in other cases (marked by colons), such an approach is clearly over-simplistic and the values are only intended to be illustrative. Estimates of the helium fraction from the line at 5015Å in both stars and from the line at 4713Å for κ Ori (both for zero microturbulence) are not given, as the strength of these lines implied unphysically large values for a strict linear extrapolation, while allowing for line saturation (where $W_\lambda \propto y^{1/2}$) yielded typically $y \gtrsim 0.5$.

Table 1. Dependence of derived atmospheric parameters of our target stars on assumed helium fraction.

	ϵ Ori		κ Ori	
y	$T_{\rm eff}$	$\log g$	$T_{\rm eff}$	$\log g$
0.1	29000	3.06	27500	3.00
0.2	28500	3.04	27000	2.92

6. Discussion

The observed and theoretical spectra (presented in Figs. 3 and 4) indicate that there is better agreement when a non-zero microturbulence is adopted. This is apparent, for example, in the triplet lines at 4713 & 4471Å. Additionally, more consistent abundance estimates for different lines in a given stellar spectrum are obtained when microturbulence is included – see Table 2. For example, previously the most 'problematic' line was probably that at 4713Å, whose theoretical line strengths were relatively insensitive to either effective temperature or gravity over the range of values considered here. As theory predicted it to be much weaker than is observed, the only way to obtain agreement was to invoke improbably large helium fractions. However, by including microturbulence, it now becomes possible to achieve acceptable fits for near-normal helium fractions. Other lines (such as 4026 & 4922Å), which had previously been fitted reasonably satisfactorily with zero microturbulence and enhanced helium fractions, can now also be reproduced with normal, or near-normal, values of y. Indeed, by assuming a zero microturbulence, helium fractions from 0.09 to well in excess of 0.4 are obtained for both stars. In contrast, by assuming a micro-

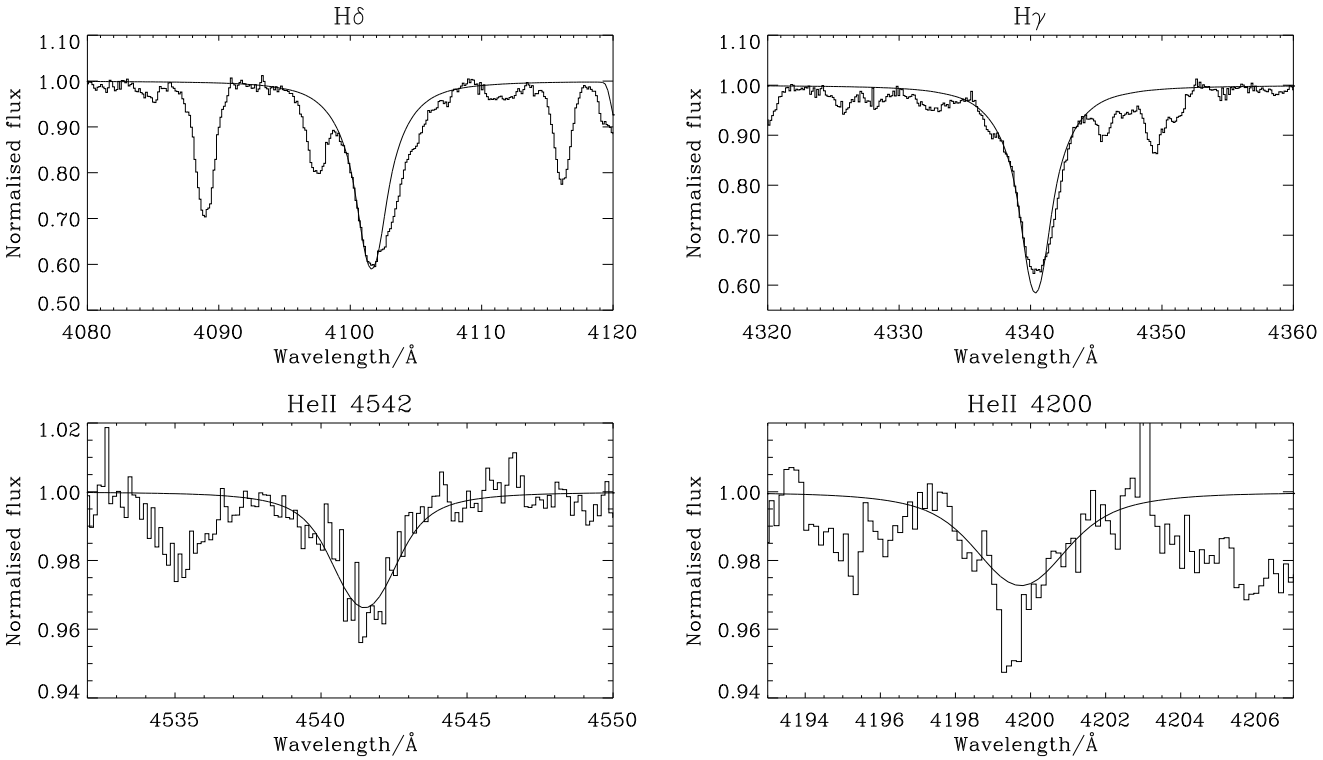

Fig. 2. Non-LTE fits for H I & He II in κ Ori. The lines shown are those which were used as the primary atmospheric parameter indicators. The theoretical profiles are for atmospheric parameters; $T_{\rm eff}$=27500 K, log g=3.00, y=0.1, v_t=12 kms^{-1}. However, the profiles for v_t=0 kms^{-1} were almost identical. The wings of Hδ contain N III lines at 4097.3 & 4103.4Å and O II lines at 4103.0, 4104.7, 4105.0 & 4106.0Å. The He II line at 4200Å is also affected by absorption due to a N III line.

Table 2. Helium fractions, y, implied by different He I lines. For each target, we give two estimates for y; viz. that determined from an analysis performed with v_t=0 kms^{-1}, and that determined using a value determined from the metal lines. In some cases the strength of the line led to an unphysically large value for the helium fraction, and y-estimates are not given – see text for further discussion.

		He I		ϵ Ori.		κ Ori.	
λ	f	Transition		v_t=0	v_t=12	v_t=0	v_t=12
5047	0.008	$1s2p$ – $1s4s$	2^1P – 4^1S	0.1	0.08†	0.15	0.1
4437	0.003	$1s2p$ – $1s5s$	2^1P – 5^1S	0.09†	0.08†	0.1	0.09†
4387	0.0436	$1s2p$ – $1s5d$	2^1P – 5^1D	0.09†	0.09†	0.1	0.1
4922	0.122	$1s2p$ – $1s4d$	2^1P – 4^1D	0.2	0.1	0.4:	0.1
5015	0.151	$1s2s$ – $1s3p$	2^1S – 3^1P	—	0.3:	—	0.3:
4713	0.012	$1s2p$ – $1s4s$	2^3P – 4^3S	0.4:	0.1	—	0.2
4026	0.047	$1s2p$ – $1s5d$	2^3P – 5^3D	0.2	0.1	0.2	0.15
4471	0.125	$1s2p$ – $1s4d$	2^3P – 4^3D	0.4:	0.2	0.4:	0.2

† indicates a small extrapolation outside our grid - estimates should be useful.
: indicates a significant extrapolation outside our grid - estimates are purely illustrative.

turbulence deduced from the silicon lines, ten (out of sixteen) estimates are between 0.08 and 0.1 (i.e. effectively normal) with other values being 0.3 or less. Hence our principal conclusion is that the adoption of a realistic microturbulent velocity leads both to better and more consistent fits and to an approximately normal helium abundance in both stars.

We also believe that our other atmospheric parameters ($T_{\rm eff}$, log g and v_t) are improvements upon previously published values because of the high quality of the spectral data and the modifications introduced to the line profile computations. As discussed previously, the introduction of a microturbulent velocity has no *direct* effect on the estimates of effective temperature and logarithmic gravity. However, since the use of a non-zero microturbulence leads to a lower estimate of the helium fraction and since $T_{\rm eff}$ and log g are dependent upon y, there is an *indirect* dependence. In Table 3, we list our best estimates of the atmospheric parameters, together with error estimates. To aid the subsequent discussion, in Fig. 5 we show for κ Ori, the

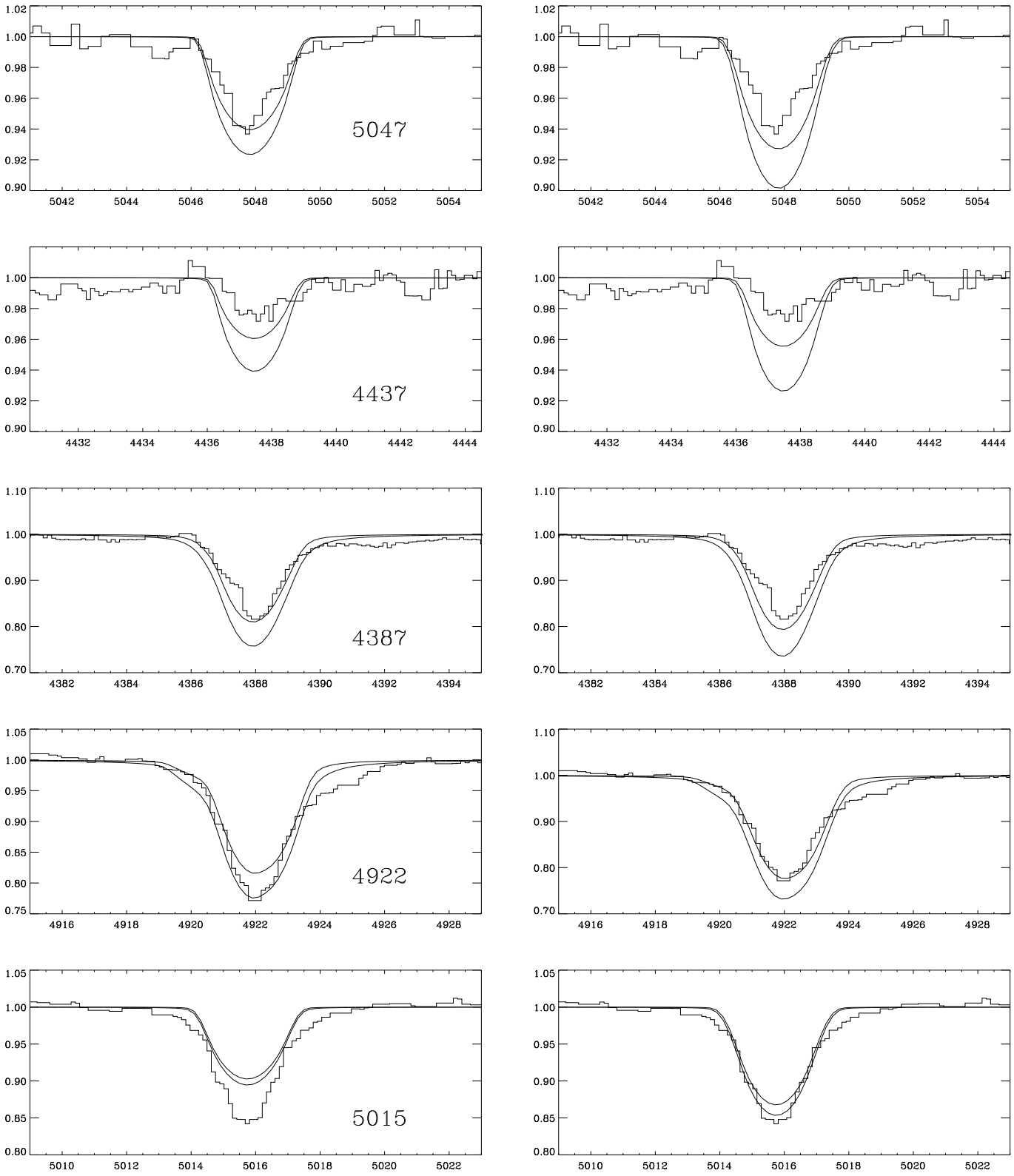

Fig. 3a. Observed profiles and non-LTE calculations for singlet He I in ϵ Ori. The latter are for atmospheric parameters $T_{\rm eff}$=29000 K, log g=3.06, y=0.1 and $T_{\rm eff}$=28500 K, log g=3.04, y=0.2. Theoretical profiles for v_t=0 kms^{-1} and v_t=12 kms^{-1} are shown on the left and right hand side, respectively and are in order of increasing oscillator strength. The absorption in the red wing of 4922 is due to O II and there is also a diffuse interstellar band bluewards of the He I line at 4437Å.

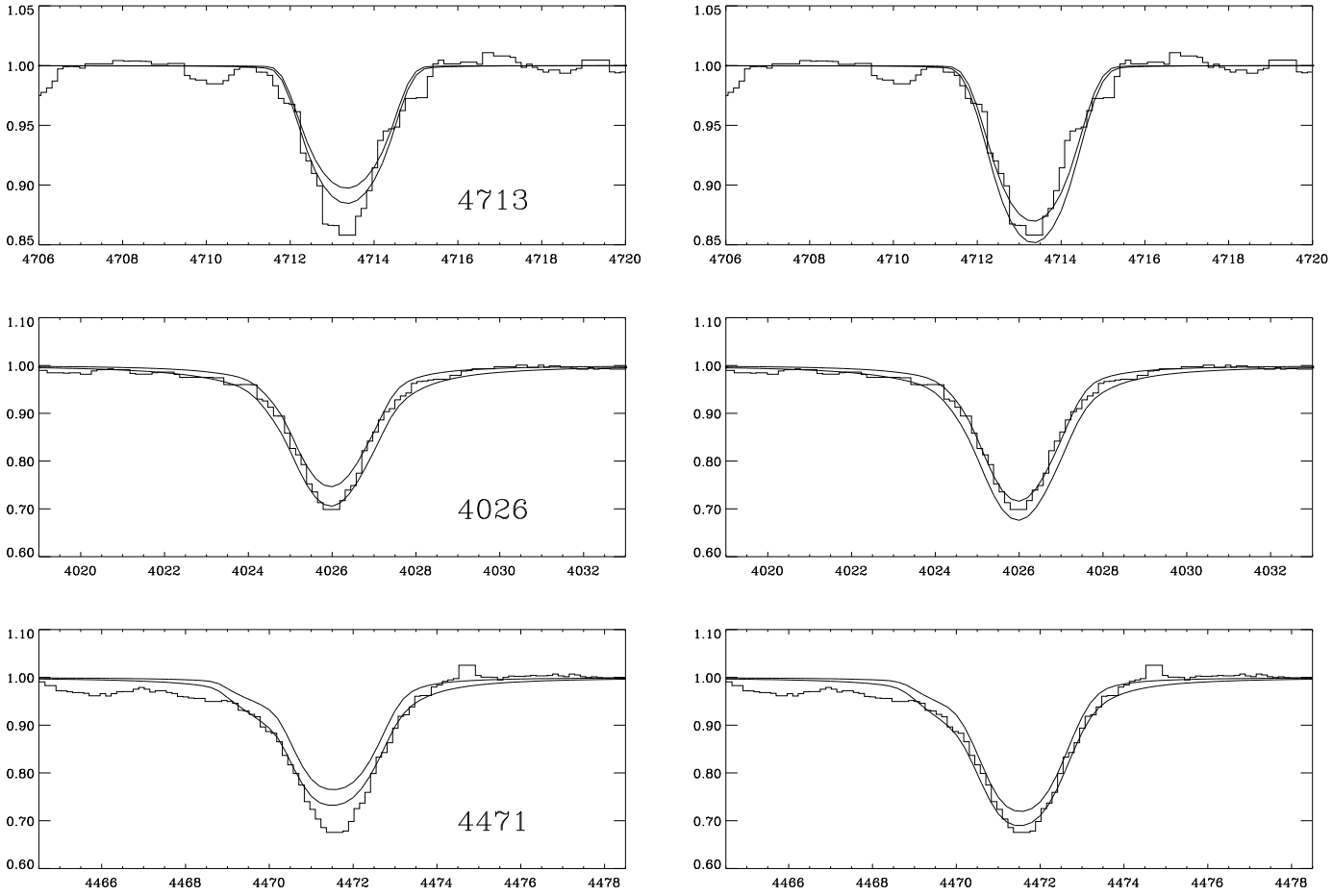

Fig. 3b. As for Fig. 3a. – for the triplet lines of He I in ϵ Ori.

points in the atmosphere where the line cores achieve an optical depth of unity.

As we have already mentioned, Voels et al. (1989) proposed that the lines of He I may be subject to the generalized dilution effect, whereby various level populations are enhanced as a result of sphericity. They suggested that this is most significant for the 2^3S level, followed by 2^1S, 2^3P and 2^1P in order of decreasing importance, the effect also decreasing for higher lying states. They suggested that those He I lines forming deepest in the atmosphere should provide the most reliable y-estimates, and used this logic in selecting the He I lines with the lowest oscillator strengths for use as helium abundance indicators. Inspection of Table 2 shows that our results for zero microturbulence fit this general picture; 4437Å (2^1P – 5^1S) and 4387Å (2^1P – 5^1D) giving normal helium abundances, while 5015Å (2^1S – 3^1P) is very discrepant. We can also see that, at these temperatures, 4713Å (recommended by Voels et al. at higher temperatures), does *not* provide consistent y-estimates compared to 4387Å. Furthermore, the lines 5047 and 4387Å, used by Smith & Howarth, give significantly lower helium abundances than the triplets, and are not seriously affected by microturbulence. Whether or not the neglect of atmospheric extension and sphericity play a significant role in determining the perceived abundance pattern is unclear, since neither κ Ori nor ϵ Ori are particularly luminous supergiants, with pressure scale heights of order $10^{-3}R_\star$. Nevertheless it is perhaps significant that 5015Å (2^1S – 3^1P) gives anomalously high helium abundances even when microturbulence is included.

Table 3. Adopted atmospheric parameters.

	$T_{\rm eff}$/K	$\log g$	y	v_t/kms^{-1}
κ Ori	27500 $\pm$1000	3.00$\pm$0.1	0.1 $\pm$0.03	12 $\pm$3
ϵ Ori	29000 $\pm$1000	3.06$\pm$0.1	0.1 $\pm$0.03	12 $\pm$3

Table 2 also demonstrates another problem not completely removed by the introduction of microturbulence, namely that the triplet transitions give systematically higher helium abundances than the singlets (we exclude 5015Å). This may be related to the neglect of line blocking in the n=2 continua of neutral helium, which would be most important for the metastable 2^3S state as discussed by Lennon & Dufton (1989). It seems unlikely that blocking in the ground state continuum could be an important factor given the very low flux levels in this spectral region for B-type supergiants.

As pointed out in the introduction, the use of microturbulence is almost ubiquitous in spectroscopic stellar analyses.

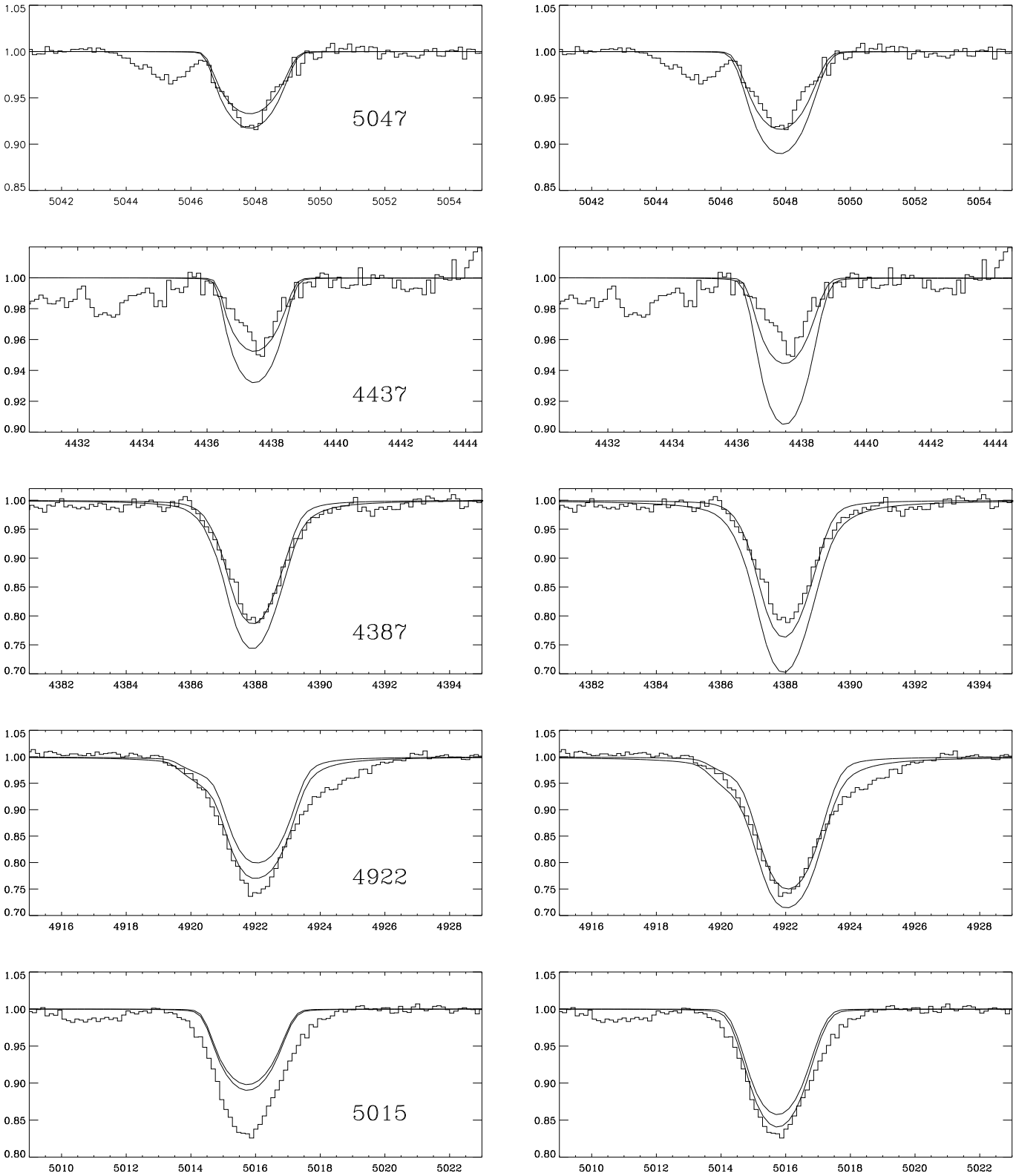

Fig. 4a. Observed profiles and non-LTE calculations for singlet He I in κ Ori. The latter are for atmospheric parameters $T_{\rm eff}$=27500 K, log g=3.00, y=0.1 and $T_{\rm eff}$=27000 K, log g=2.92, y=0.2. Theoretical profiles for v_t=0 kms^{-1} and v_t=12 kms^{-1} are shown on the left and right hand side, respectively and are in order of increasing oscillator strength.

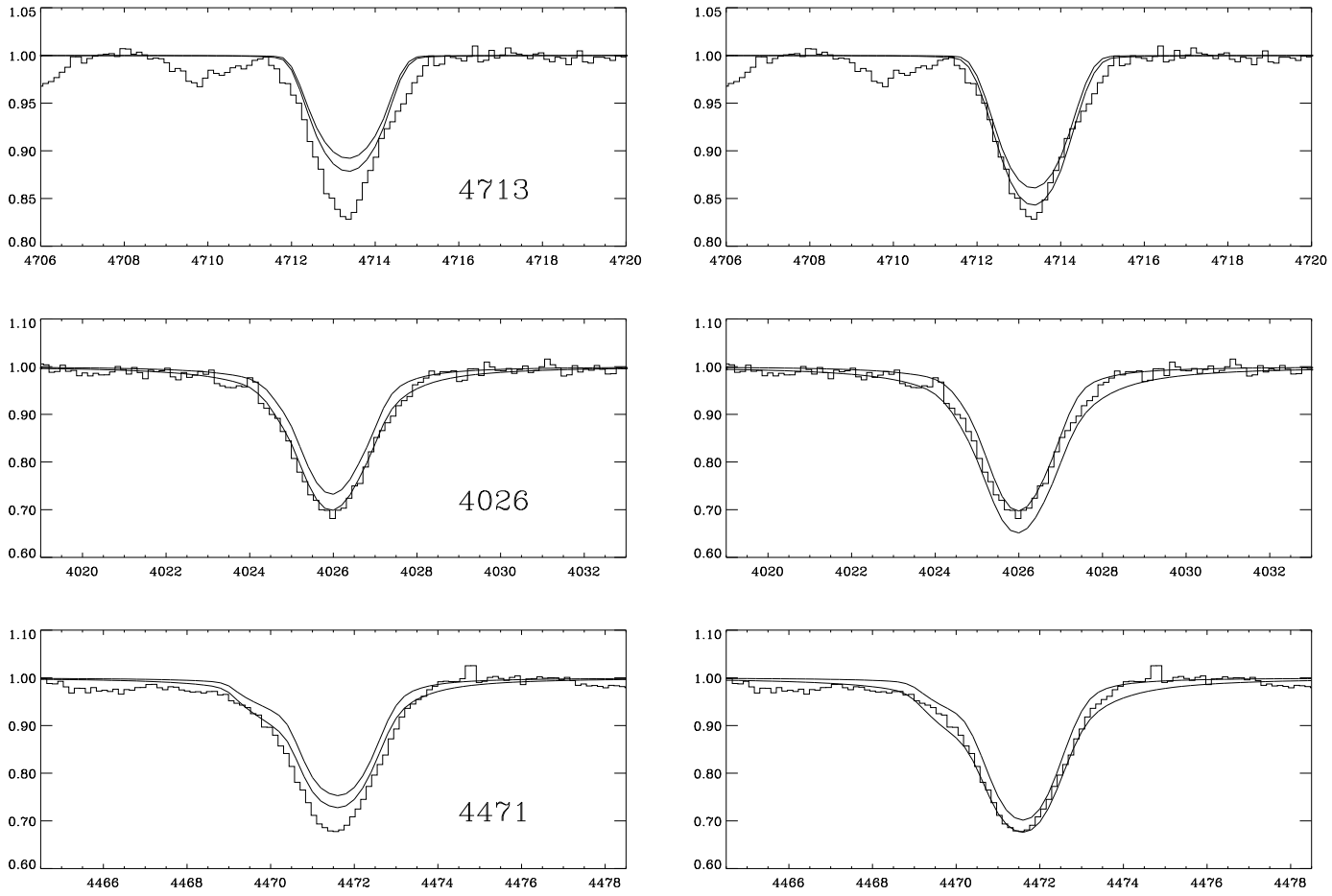

Fig. 4b. As for Fig. 4a. – for the triplet lines of He I in κ Ori.

However, in spite of the evidence in support of the reality of microturbulent velocity fields in stellar atmospheres, one must remain cautious. B-type supergiants have appreciable mass loss rates (Prinja et al. 1990), and the resultant velocity fields above the stellar photosphere can affect line profiles in such a way as to mimic microturbulence if a simple hydrostatic analysis is applied (Kudritzki 1992, Lamers & Achmad 1994). Indeed Lamers & Achmad show that velocity fields in the upper photosphere of an early B-type supergiant may lead to an *apparent* microturbulence of 10–15 kms^{-1}. They argue that microturbulent velocity values such as those derived here are thus vastly overestimated, the derived values being the sum of a real (possibly zero) microturbulent velocity and a contribution due to the neglect of the dynamic nature of the supergiant photosphere. However, these calculations assumed LTE level populations and opacities and LTE analyses of such supergiants can result in much higher values of microturbulence (see Sect. 2). Additionally, main sequence B-type stars also exhibit evidence for significant microturbulent velocities and they have mass loss rates which are approximately 2 orders of magnitude lower than supergiants (Najarro et al 1996). [In terms of outflow velocity in the photosphere, one might expect the lower mass loss rate to be partly compensated for by the smaller radius, however this is in turn partially offset by the higher surface gravities and densities of main sequence stars.] We note that the star ϵ CMa (B2 II) considered by Najarro et al., was also investigated by Gies & Lambert (1992) who derived a microturbulent velocity of 11.5$\pm$2.5 kms^{-1} from a non-LTE analysis of its metal lines.

The additional broadening introduced by the use of a non-zero microturbulence might affect the estimation of projected rotational velocities. This effect would be particularly interesting in the case of early O-type stars where slow rotators are rarely observed (see, for example, Penny 1996). However, the effect would only be significant for slowly rotating stars observed at high spectral resolution (i.e. with an instrumental width less than or approximately equal to the inferred microturbulence) and hence we do not believe that this possible additional intrinsic broadening should significantly affect previous investigations of stellar rotational velocities.

Whether our results can be explained solely by a macroscopic velocity field (wind) or whether some microturbulent contribution is still required, is unclear. It is an issue however which has obvious and potentially far-reaching implications for stellar atmospheres and the winds of hot stars (for example see Hubeny et al. 1991). If microturbulence is present then it will have greatest impact in the transition region between the near

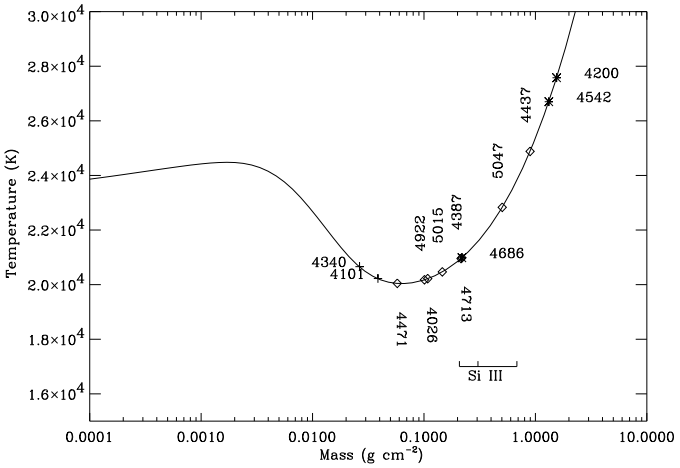

Fig. 5. Plot of temperature versus mass (depth), showing the points at which the line cores of the lines of interest attain an optical depth of unity; the He I singlet lines (diamonds: 5047, 5015, 4922, 4437 and 4387), He I triplets (diamonds: 4713, 4471 and 4026), He II lines (asterisks: 4686, 4542 and 4200) and H I lines (crosses: 4340 and 4101). The depths of formation of the Si III triplet used to determine the microturbulence are also shown. These data are for our final κ Ori model with $T_{\rm eff}$ = 27500 K, $\log g$ = 3.0, y = 0.1 and v_t=12 kms^{-1}. The optical continuum forms only a little further out than the He II lines.

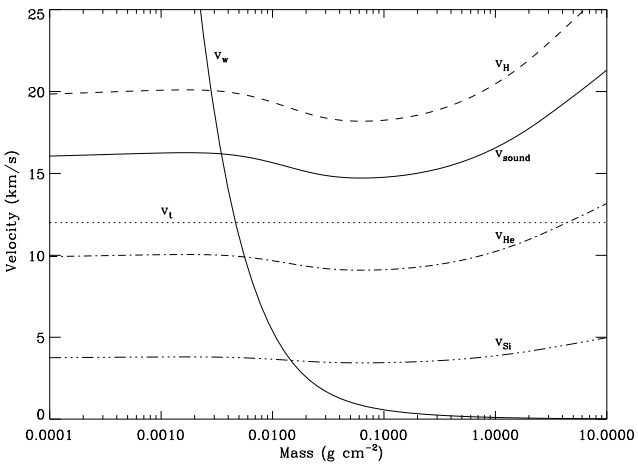

Fig. 6. For the same model as in Fig. 5 we plot some relevant velocities as follows; hydrogen thermal velocity ($v_{\rm H}$), helium thermal velocity ($v_{\rm He}$), silicon thermal velocity ($v_{\rm Si}$), adiabatic sound speed ($v_{\rm sound}$), microturbulent velocity ($v_{\rm t}$). For illustration, we also show the outflow velocity ($v_{\rm w}$) implied by the continuity equation and assuming a radius of 30 solar radii for κ Ori and a mass loss rate of $10^{-6} M_{\odot}$/yr.

hydrostatic layers in the atmosphere and the sonic point, where the thermal Doppler width is decreasing and before the wind outflow velocity begins to dominate (see Fig. 6). Should such microturbulent velocities be comparable to either ion thermal velocities or the sound speed in this region, then there will clearly be a significant effect on the line formation, structure and even the line force. We cannot address these issues in the present paper, using as we do hydrostatic equilibrium models. Certainly one can estimate an outflow velocity for a given mass loss rate and stellar radius, just using the equation of continuity, and this is also plotted in Fig. 6. However the low velocities implied by this procedure (for example 1 kms^{-1} for the line core of 4471Å), are certainly unreliable as the density structure will be drastically altered by the velocity field (see Najarro et al. 1996, Santolaya-Ray et al. 1997 and Kudritzki 1997). Test calculations for a model applicable to κ Ori indicate that outflow velocities in the He I line formation regions may in fact be of order 10 kms^{-1}, but detailed analysis of the spectrum using non-LTE calculations and hydrodynamical models are required to investigate the full implications for the implied properties of supergiants. However, whatever the physical origin of the additional broadening (and hence line desaturation) that is incorporated here via a microturbulent velocity, we do not believe that it significantly affects the main conclusions of this paper regarding the derived helium abundances.

The main conclusion of this paper is that helium abundances of hot supergiants are over-estimated when the results of non-LTE hydrostatic equilibrium model atmosphere analyses are indiscriminately applied to all available He I lines. Contrary to previous results (Lennon et al. 1991, Kudritzki et al. 1987), we find close to solar helium abundances for the two Galactic supergiants κ Ori and ϵ Ori. This is an important result (which must of course be verified) since these two stars are often considered to be *normal* supergiants (but see below). If these objects did have significant helium overabundances then an obvious explanation would be that they are post-RSG (red supergiant) core helium burning stars. This scenario now appears to be ruled out, which agrees with the results of Venn (1995) who finds that slightly less massive Galactic A-supergiants have CNO abundances which are also inconsistent with the blue loop scenario for massive star evolution at solar metallicity. In addition, from Table 2, we note that there is some slight evidence that κ Ori is marginally enhanced in helium compared to ϵ Ori. While the difference is well within our error bars this may be significant since ϵ Ori belongs to a class of supergiants with morphologically moderate anomalies, being nitrogen weak (Walborn 1976). We would interpret this as implying that κ Ori is in fact slightly nitrogen, and helium, rich. This would also be consistent with Venn's results since moderate CN anomalies were found for some A-supergiants, and is attributed to mixing processes occuring on the main sequence.

One can also speculate that the helium enrichments in O-type stars discussed by Herrero et al. (1992) may be due, at least partly, to the neglect of velocity fields. This possibility was also suggested by Schaerer & Schmutz (1994) and is well worth investigating since there is a general trend of increasing helium abundance with luminosity class in the Herrero et al. sample. These authors considered only the He I lines at 4471, 4922 to 4387Å but, recognising that the dilution effect was present in their results, they concentrated on 4922 and 4387Å. However, they gave greatest weight to the former which, if our results can be extended to O-type stars, would imply that helium abundances may still be overestimated. Indeed, since submission of

this paper, we have become aware of work by Smith (1997) which shows that the inclusion of microturbulence in the non-LTE analysis of late O-type supergiants *does* lead to improvements in line profile fits and a reduction in the estimated helium fractions for these stars.

Finally, we emphasize that for those stars with microturbulent values of the order discussed here (which may include some main-sequence stars), it is important to include this parameter in the calculation of the level populations.

Acknowledgements. Observational data were obtained at the 3.6m telescope at La Silla. We are grateful to the staff at the observatory for their assistance. Data reduction was performed in Munich and on the PPARC funded Northern Ireland STARLINK node, and some of the model atmosphere programs were made available through the PPARC supported Collaborative Computational Project No. 7. We would also like to acknowledge useful discussions with, and test calculations by, Rolf Kudritzki and Paco Najarro.

DJL is grateful for financial support from the Bundesminister für Forschung und Technologie under grant 010 R 90080.

NDME holds a post-graduate studentship from the Department of Education for Northern Ireland.

We are grateful to the British Council and the Deutsche Akademischer Austauschdienst for funding an ARC program of working visits between Munich and Belfast.

References

Butler K., 1984, Ph.D. Thesis, University of London
Dufton P.L., 1972, A&A 16, 301
Fliegner J., Langer N., Venn K.A., 1996, A&A 308, L13
Gabler R., Gabler A., Kudritzki R.-P., Puls J., Pauldrach A., 1989, A&A 226, 162
Giddings J.R., 1981, Ph.D. Thesis, University of London
Gies D.R., Lambert D.L., 1992, ApJ 387, 673
Groenewegen M.A.T., Lamers H.J.G.L.M., 1989, A&AS 79, 359
Hardorp J., Scholz M., 1970, ApJS 19, 193
Haser S.M., Lennon D.J., Kudritzki R.-P. et al., 1995, A&A 295, 136
Herrero A., Kudritzki R.-P., Vilchez J.M. et al., 1992, A&A 261, 209
Howarth I.D., Murray M.J., 1991, Starlink User Note No. 50, Rutherford Appleton Laboratory, UK
Hubeny I., Heap S.R., Altner B., 1991, ApJL 377, L33
Kamp L.W., 1978, ApJS 48, 415
Kilian J., Becker S.R., Gehren T., Nissen P.E., 1991, A&A 244, 419
Kudritzki R.-P., 1992, A&A 266, 395
Kudritzki R.-P., 1997, in Proceedings of the 8th Canary Islands Winter School, *in press*
Kudritzki R.-P., Groth H.G., Butler K. et al., 1987, in ESO Workshop on SN1987A, ed. I.J. Danziger, p39.
Lamers H.J.G.L.M., 1972, A&A 17, 34
Lamers H.J.G.L.M., Achmad L., 1994, A&A 291, 856
Langer N., Maeder A., 1995, A&A 295, 685
Lennon D.J., 1994, Space Sci. Rev. 66, 127
Lennon D.J., 1997, A&A 317, 871
Lennon D.J., Dufton P.L., 1986, A&A 155, 79
Lennon D.J., Dufton P.L., 1989, A&A 225, 439
Lennon D.J., Kudritzki R.-P., Becker S.R. et al., 1991, A&A 252, 498
Maeder A., 1994, Space Sci. Rev. 66, 349
Maeder A., Meynet G., 1989, A&A 210, 155
McCarthy J.K., Kudritzki R.-P., Lennon D.J., Venn K.A., Puls J., 1997, ApJL *in press*
McErlean N.D., Lennon D.J., Dufton P.L., 1997, *in preparation*
Mihalas D., 1972, ApJ 177, 115
Najarro F., Kudritzki R.-P., Cassinelli J.P., Stahl O., Hillier J., 1996, A&A 306, 892
Penny L.R., 1996, ApJ 463, 737
Peterson D.M., Scholz M., 1971, ApJ 163, 51
Ponz D., Brinks E., 1986, ESO-messenger 43, 31
Prinja R.K., Barlow M.J., Howarth I.D., 1990, ApJ 361, 607
Santolaya-Rey A.E., Puls J., Herrero A., 1997, A&A *in press*
Schaerer D., Schmutz W., 1994, A&A 288, 231
Smartt S.J., Dufton P.L., Lennon D.J., 1997, A&A *in press*
Smith K.C., Howarth I.D., 1994, A&A 290, 868
Smith K.C., 1997, *private communication*
Snijders M.A.J., Lamers H.J.G.L.M., 1975, A&A 41, 245
Struve O., Elvey C., 1934, ApJ 79, 409
Venn K.A., 1995, ApJ 449, 839
Voels S.A., Bohannan B., Abbott D.C., Hummer D.G., 1989, ApJ 340, 1073
Walborn N.R., 1976, ApJ 205,419

This article was processed by the author using Springer-Verlag LaTeX A&A style file *L-AA* version 3.